(12) INTERNATIONAL APPLICATION PUBLISHED UNDER THE PATENT COOPERATION TREATY (PCT)

(19) World Intellectual Property Organization
International Bureau

(43) International Publication Date
14 August 2008 (14.08.2008)

PCT

(10) International Publication Number
WO 2008/096344 A2

(51) International Patent Classification:
G03H 1/08 (2006.01) *G03H 1/02* (2006.01)
H04N 13/00 (2006.01)

(21) International Application Number:
PCT/IL2008/000142

(22) International Filing Date: 3 February 2008 (03.02.2008)

(25) Filing Language: English

(26) Publication Language: English

(30) Priority Data:
60/899,408 5 February 2007 (05.02.2007) US

(71) Applicant *(for all designated States except US)*: **BEN-GURION UNIVERSITY OF THE NEGEV RESEARCH AND DEVELOPMENT AUTHORITY** [IL/IL]; P.O.B. 653, 84105 Beer Sheva (IL).

(72) Inventors; and

(75) Inventors/Applicants *(for US only)*: **ROSEN, Joseph** [IL/IL]; 17 Livne Street, 84965 Omer (IL). **SHAKED, Natan, Tzvi** [IL/IL]; 13/16 Ya'akov Cohen Street, 84374 Beer Sheva (IL). **STERN, Adrian** [IL/IL]; 3 Hashita Street, 84965 Omer (IL).

(74) Agents: **LUZZATTO, Kfir** et al.; P.O. Box 5352, 84152 Beer Sheva (IL).

(81) Designated States *(unless otherwise indicated, for every kind of national protection available)*: AE, AG, AL, AM, AO, AT, AU, AZ, BA, BB, BG, BH, BR, BW, BY, BZ, CA, CH, CN, CO, CR, CU, CZ, DE, DK, DM, DO, DZ, EC, EE, EG, ES, FI, GB, GD, GE, GH, GM, GT, HN, HR, HU, ID, IL, IN, IS, JP, KE, KG, KM, KN, KP, KR, KZ, LA, LC, LK, LR, LS, LT, LU, LY, MA, MD, ME, MG, MK, MN, MW, MX, MY, MZ, NA, NG, NI, NO, NZ, OM, PG, PH, PL, PT, RO, RS, RU, SC, SD, SE, SG, SK, SL, SM, SV, SY, TJ, TM, TN, TR, TT, TZ, UA, UG, US, UZ, VC, VN, ZA, ZM, ZW.

(84) Designated States *(unless otherwise indicated, for every kind of regional protection available)*: ARIPO (BW, GH, GM, KE, LS, MW, MZ, NA, SD, SL, SZ, TZ, UG, ZM, ZW), Eurasian (AM, AZ, BY, KG, KZ, MD, RU, TJ, TM), European (AT, BE, BG, CH, CY, CZ, DE, DK, EE, ES, FI, FR, GB, GR, HR, HU, IE, IS, IT, LT, LU, LV, MC, MT, NL, NO, PL, PT, RO, SE, SI, SK, TR), OAPI (BF, BJ, CF, CG, CI, CM, GA, GN, GQ, GW, ML, MR, NE, SN, TD, TG).

Published:
— *without international search report and to be republished upon receipt of that report*

WO 2008/096344 A2

(54) Title: A METHOD AND SYSTEM FOR OBTAINING DIGITAL HOLOGRAMS IN A SINGLE CAMERA SHOT USING WHITE-LIGHT

(57) Abstract: The present invention is a method and a system for obtaining a digital hologram of a three-dimensional (3-D) scene. The method is preformed by illuminating the scene with incoherent white-light, recording multiple projections of the 3-D scene, and finally, computer processing of the projections by the performance of a predetermined sequence of mathematical operations. The method and the system of the current invention are characterized in that a microlens array (MLA) is used to create the multiple projections in an image plane which is projected onto the imaging sensor of a camera. This allows the obtaining of all of the multiple projections in a single camera shot.

A METHOD AND SYSTEM FOR OBTAINING DIGITAL HOLOGRAMS IN A SINGLE CAMERA SHOT USING WHITE-LIGHT

Field of the Invention

The present invention relates to the field of holograms, specifically this invention relates to a method and system for obtaining digital holograms, under spatially incoherent white-light illumination and in a single camera shot.

Background of the Invention

Conventional holography involves the acquisition of an interference pattern created by interfering beams coming from a three dimensional (3-D) scene and a reference beam. The creation of this interference pattern requires a meticulous stability of the optical system, high intensity and narrow bandwidth of the light source used. These strict requirements inhibit the usage of conventional holography for many practical applications.

A partial solution to these problems is suggested by the scanning holography method [1]. According to this method, a digital Fresnel hologram can be obtained, under spatially incoherent illumination conditions, by scanning the 3-D scene with a pattern of a Fresnel zone

plate, so that the light intensity at each scanning position is integrated by a point detector. However, the scanning process in this method is performed by mechanical movements, and thus the hologram acquisition is relatively slow. In addition, this hologram technique is not suitable for moving objects.

In order to avoid these mechanical movements, another method for obtaining digital Fresnel holograms, named FINCH (Fresnel incoherent correlation holography), is proposed in Ref. [2]. According to this method, the spatially incoherent light coming from the 3-D scene propagates through a diffractive optical element (DOE) and is recorded by a camera. Then, three different holograms, each with a different phase factor of the DOE, are recorded sequentially and superposed in the computer into a digital Fresnel hologram.

A fundamentally different solution is suggested in Refs. [3,4]. According to the methods presented there, the 3-D scene is illuminated by spatially incoherent white light and viewed from multiple angles. For each view angle, the projection of the 3-D scene is acquired by a camera and processed in the computer. The result is a 2-D complex function which represents a digital hologram of the 3-D scene. This function can be encoded into a computer generated hologram (CGH) with real and positive transparency values. Then, the recorded 3-D scene can be reconstructed by

illuminating the CGH transparency with a plane wave. Alternatively, a digital holography technique can be employed in order to digitally reconstruct the 3-D scene.

In spite of the great advantages presented by the above described methods and their potential of making holography attractive for many practical applications, the 3-D scene recording process in these methods is still considered long and quite complicated. This occurs because the camera has to be repositioned many times in order to obtain enough 3-D scene projections, required for the synthesis of a hologram with an acceptable resolution and also because the former methods are not suitable for holography of moving objects.

It is therefore an object of this invention to provide an improved method for obtaining digital holograms.

Other objects and advantages of present invention will appear as description proceeds.

Summary of the Invention

In a first aspect, the present invention is a method of obtaining a digital hologram of a 3-D scene comprising the steps of: (i) illuminating the scene with incoherent white-light; (ii) recording multiple projections of the 3-D

scene; and (iii) computer processing of the projections by the performance of a predetermined sequence of mathematical operations. The method of the current invention is characterized in that a microlens array (MLA) is used to create the multiple projections in its image plane. This MLA image plane is projected onto the imaging sensor of a camera. This allows the obtaining of all of the multiple projections in a single camera shot.

In one embodiment, the predetermined sequence of mathematical operations comprises the steps of (i) cutting the single shot image received from the camera into a set of projections of the 3-D scene; (ii) centering the projections on the same reference point; (iii) multiplying the centered projections by linear phase functions; and (iv) summing each of the multiplied results into a single complex value. These steps yield a complex matrix which represents a digital hologram.

In another embodiment the predetermined sequence of mathematical operations comprises the digital incoherent modified Fresnel hologram (DIMFH) method.

In another embodiment the predetermined sequence of mathematical operations comprises the digital incoherent protected correlation hologram (DIPCH) method.

In another aspect the present invention is a system for obtaining a digital hologram of a 3-D scene comprising a source of incoherent white-light; a collimating lens; a microlens array (MLA); a focusing lens; a camera; and a computer. The system is characterized in that the MLA creates multiple images of the scene in the image plane of said MLA. The image plane is projected by the focusing lens onto the imaging sensor of the camera, thereby allowing the obtaining of all of the multiple projections of the scene in a single camera shot. Next, the multiple projections are transferred to the computer, and finally a predetermined sequence of mathematical operations is preformed on these projections to obtain the digital hologram.

Brief Description of the Drawings

The above and other characteristics and advantages of the invention will be more readily apparent through the following examples, and with reference to the appended drawings, wherein:

Fig. 1 schematically shows the integral holography (IH) optical system used for capturing the multiple projections of the 3-D scene;

Fig. 2 schematically illustrates one embodiment of the IH processing stage;

Fig. 3 is a cross section of part of the optical system shown in Fig. 1;

Fig. 4 is a contrast-inverted picture showing several projections taken from different parts of the microlens array (MLA) image plan captured by the camera;

Fig. 5A is a contrast-inverted picture showing the magnitude of the Fourier hologram obtained after performing the processing stage on the captured projections;

Fig. 5B is a contrast-inverted picture showing the phase of the Fourier hologram obtained after performing the processing stage on the captured projections;

Fig. 5C is a contrast-inverted picture showing the reconstruction of the hologram at the best focus distance of the letter 'I';

Fig. 5D is a contrast-inverted picture showing reconstruction of the hologram at the best focus distance of the letter 'H';

Fig. 6 is a schematic illustration of the projection onto the constraint sets (POCS) algorithms for finding the point spread function (PSF) used for the digital incoherent protected correlation hologram (DIPCH);

Fig. 7A shows the generating constrained random PSFs used for the 1-D DIPCH;

Fig. 7B shows the generating constrained random PSFs used for the 2-D DIPCH.

Detailed Description of the Invention

Description of the method

The overall process of obtaining the hologram according to the present invention can be divided into two main stages: the recording stage and the processing stage. In the recording stage, multiple projections of the 3-D scene are captured in a single camera shot, whereas in the processing stage, mathematical operations are performed on these projections in order to yield a digital two-dimensional (2-D) hologram or one-dimensional (1-D) hologram.

Fig. 1 shows the integral holography (IH) optical system of the present invention used for capturing the multiple projections of the 3-D scene 10, which is illuminated by white-light. As shown in this figure, a microlens array (MLA) 14 is employed in order to create these multiple projections. A plano-convex lens 12, positioned at a distance of its focal length f_1 from the 3-D scene 10 and attached to the MLA 14, is used in order to collimate the light coming from the 3-D scene 10 and thus to increase the number of microlenses participating in the process. In fact, the plano-convex lens 12 and the MLA 14 together can be considered as a new equivalent MLA 14' which sees the 3-D scene 10 at a larger distance from the MLA 14 than the distance to the scene without the plano-convex lens 12. A spherical lens 18, with a focal length of f_2, projects the MLA image plane 16 onto the

camera 20 with the magnification of $-z_2/z_1$. Then, the camera 20 captures the entire MLA image plane 16 in a single shot and sends it to the computer 22 for the processing stage.

Assume that the MLA contains $(2K+1)\times(2K+1)$ microlenses. The microlenses are numbered by the indices m and n, so that the middle microlens is denoted by $(m,n) = (0,0)$, the upper right microlens by $(m,n) = (-K,-K)$ and the lower left microlens by $(m,n) = (K,K)$. Let $P_{m,n}(X_p,Y_p)$ be the projection created by the (m,n)-th microlens, where X_p and Y_p are the axes of this projection. The MLA image plane 16, captured by a single camera shot in the recording stage of the present invention, consists of an array of small elemental images, each obtained by a different microlens in the MLA and thus representing another projection $P_{m,n}(X_p,Y_p)$ of the 3-D scene 10 from a different point of view.

Fig. 2 illustrates one method of carrying out the processing stage of the present invention. After capturing the MLA image plane from the CCD camera in stage 100, each projection of the MLA image is cut, as shown in stages 102 and 104, after detecting the first and last elemental image in each row of the MLA plane. In step 106 each of the elemental images taken from the MLA image plane is centered on the same reference point, which yields a set of new projections $P^c_{m,n}(X^c_p,Y^c_p)$, shown in stage 108. As a

result of this centering the radial distance from the reference point is the same for all of the projections. Afterward, as seen in stage 110, each of the centered projections is multiplied by a linear phase function, which is dependent on the relative position of the projection in the entire projection set. Finally, in stage 112, the result of each multiplication is summed up into a single complex value. Mathematically, this process can be described as follows:

$$H_{m,n} = \iint P^c_{m,n}(X^c_p, Y^c_p) E_{m,n}(X^c_p, Y^c_p) dX^c_p dY^c_p, \quad (1)$$

where:

$$E_{m,n}(X^c_p, Y^c_p) = \exp[-j(2\pi b / D)(mX^c_p + nY^c_p)], \quad (2)$$

where D is the distance between the centers of two adjacent microlenses in the array and b is an adjustable parameter. The process is performed for each of the centered projections, which yields, as shown in stage 114, a 2-D complex matrix H representing the digital 2-D Fourier hologram of the 3-D scene. This hologram is equivalent to the complex amplitude in the rear focal plane of a spherical lens due to a coherent light diffracting from the same 3-D scene and propagating through this lens.

Recently, Mishina et al. [5] have demonstrated a method of calculating a CGH from elemental images captured by integral photography. Their CGH is a composite of many elemental Fresnel holograms, each created by a different microlens. Unlike the Mishina et al. [5] method, in the IH method of the present invention, each (m,n)-th pixel in the hologram is

contributed only from the (*m*,*n*)-th microlens. Therefore, the entire information of the elemental images is compressed into a matrix with a number of elements which is equal to the number of microlens. Another difference from the composite computer generated hologram (CGH) method is that according to the processing stage of the present invention, the IH hologram is of a Fourier type, and this opens many possibilities of spatial filtering and correlation on the captured images.

Equivalence between the first digital process and a digital Fourier hologram

In order to show that the complex matrix H indeed represents the digital Fourier hologram of the 3-D scene in the present invention, the mathematical relations between point (x_s, y_s, z_s) in the 3-D scene 10 and its projected point (x_p, y_p) located on the (*m*,*n*)-th projection plane (X_p, Y_p) obtained by the MLA 14 is first defined. Fig. 3 shows certain geometric relationships of the optical system shown in Fig. 1. Simple geometric relationships in this figure yield the following:

$$x_p = \frac{M(mD + x_s)}{1 - z_s / L}; \quad y_p = \frac{M(nD + y_s)}{1 - z_s / L}, \tag{3}$$

where M is the magnification of each of the microlenses in the array, L is the distance between the origin of the 3-D scene 10 and the equivalent MLA 14' (taking into account the effect of the plano-convex lens 12). By

assuming that the maximal value of z_s is much smaller than L, the approximation $(1-\alpha/\beta)^{-1} \cong 1+\alpha/\beta$, where $\alpha << \beta$, can be applied to Eq. (3) to yield:

$$x_p \cong M(mD + x_s + z_s mD/L + z_s x_s/L);\quad y_p \cong M(nD + y_s + z_s nD/L + z_s y_s/L). \quad (4)$$

As explained above, each projection $P_{m,n}(X_p, Y_p)$ is centered on the same reference point, which yields the centered projection $P^c_{m,n}(X^c_p, Y^c_p)$. Due to this centering, *MmD* and *MnD* are subtracted from x_p and y_p, respectively, in order to get x^c_p and y^c_p located on the centered projection $P^c_{m,n}(X^c_p, Y^c_p)$. This means that the point (x_s, y_s, z_s) in the 3-D scene 10 is projected to the point (x^c_p, y^c_p) in the centered projection according to the following formula:

$$x^c_p \cong M(x_s + z_s mD/L + z_s x_s/L);\quad y^c_p \cong M(y_s + z_s nD/L + z_s y_s/L). \quad (5)$$

An infinitesimal element with the size of $(\Delta x_s, \Delta y_s, \Delta z_s)$, located on the 3-D object surface at coordinates (x_s, y_s, z_s) and having the value of $h(x_s, y_s, z_s)$, is now considered. This infinitesimal element should appear on all of the centered projections planes, but at a different location on each plane. Therefore, based on Eq. (1), the amplitude distribution on the (m,n)-th centered projection plane, caused by a single source point (SSP) in the 3-D scene, is given by:

$$H^{SSP}_{m,n}(x_s, y_s, z_s) = \iint [h(x_s, y_s, z_s)\Delta x_s \Delta y_s \Delta z_s \delta(X^c_p - x^c_p, Y^c_p - y^c_p)] E_{m,n}(X^c_p, Y^c_p) dX^c_p dY^c_p$$
$$= h(x_s, y_s, z_s) E_{m,n}(x^c_p, y^c_p)\, \Delta x_s \Delta y_s \Delta z_s,$$

(6)

where δ is the Dirac delta impulse. Substituting Eqs. (2) and (5) into Eq. (6) yields:

$$H_{m,n}^{SSP}(x_s,y_s,z_s)=h(x_s,y_s,z_s)\exp\{-j(2\pi bM/D)[m(x_s+z_s mD/L+z_s x_s/L) \quad (7)$$
$$+n(y_s+z_s nD/L+z_s y_s/L)]\}\,\Delta x_s\Delta y_s\Delta z_s.$$

Taking into account the fact that the overall distribution of the hologram is a volume integral of all points on the 3-D object, the following is obtained:

$$H_{m,n}=\iiint H_{m,n}^{SSP}(X_s,Y_s,Z_s)\,dX_s dY_s dZ_s=\iiint h(X_s,Y_s,Z_s)\exp\{-j(2\pi bM/D)$$
$$\times[mX_s+nY_s+(Z_s D/L)(m^2+n^2)+(Z_s/L)(mX_s+nY_s)]\}dX_s dY_s dZ_s. \quad (8)$$

Using the continuous variables $(u/D,v/D)$ instead of the discrete variables (m,n) and assuming that $L>>2\pi Mu_{\max}\delta Z_s\delta X_s$ and $L>>2\pi Mv_{\max}\delta Z_s\delta Y_s$, where $(\delta X_s,\delta Y_s,\delta Z_s)$ is the size of the 3-D scene, and $u_{\max}$ and $v_{\max}$ are the maximal horizontal and vertical coordinate values on the Fourier plane, respectively, then the last term inside the integral of Eq. (8) can be neglected, yielding the following equation:

$$H(u,v)\cong\iiint h(X_s,Y_s,Z_s)\exp\left\{-\frac{j2\pi bM}{D^2}[uX_s+vY_s+(Z_s/L)(u^2+v^2)]\right\}dX_s dY_s dZ_s. \quad (9)$$

Eq. (9) has the same functional behavior of the complex amplitude obtained for a Fourier hologram [3] and therefore the proposed IH system indeed creates a digital Fourier hologram.

The transversal minimal distance Δx_s and the axial minimal distance Δz_s that can be resolved through the optical system are given as follows:

$$\Delta x_s = \max\{1.22\lambda L / D,\ p_c z_1 /(Mz_2)\};\qquad \Delta z_s = \Delta x_s L /(KD), \tag{10}$$

where λ is the average wavelength used ($\lambda \approx 0.5\mu m$) and p_c is the pixel size of the recording camera. The axial optical resolution given in Eq. (10) is determined by projecting the axial minimal resolved distance Δz_s on the transverse object plane of the most extreme microlens in the MLA. The parameter b is determined so that the computed Fourier hologram given by Eq. (9) maintains the maximum possible resolution of the system given by Eq. (10). Therefore, the parameter b is given as follows:

$$b = D /(MK\Delta x_s). \tag{11}$$

This embodiment of the invention will be further described and illustrated in the following example.

Example

The optical system shown in Fig. 1 was experimentally implemented. Two bright letters, 'I' and 'H', were positioned in a dark environment and

illuminated by a spatially incoherent white-light source. The size of the letters was 2 cm × 2 cm each, and the distances between them on the optical axis Z, the vertical axis Y and the horizontal axis X were 10 cm, 1 cm and 3 cm, respectively. The plano-convex lens 12, attached to the MLA 14 on the side of the 3-D scene 10, had a diameter of 10 cm and a focal length of $f_1 = 40$ cm. Therefore, the distance between the 3-D scene 10 and the MLA 14 was about 40 cm as well. A hexagonal-format MLA, 5 cm in diameter, with a pitch of 500 μm and with 115×110 microlenses was used. However, only the 65×65 middle microlenses were employed in the experiment. The focal length of each of the microlenses in the MLA 14 was $f_{MA} = 3.3$ mm. In order to project the MLA image plane 16 onto the camera 20 with the magnification factor of −2, a spherical imaging lens 18 with a focal length of $f_2 = 10$ cm was used. A CCD camera (PCO, Scientific 230XS) 20, containing 1280×1024 pixels and an 8.6×6.9 mm^2 active area, was used. Several camera planes were concatenated due to the relatively low number of pixels in the CCD camera 20 used (compared to other cameras on the market today). Note that the use of the available hexagonal-format MLA, rather than a square-format MLA, decreased the quality of the reconstruction because of the mismatch between the MLA and the square-format grid of the computer. Therefore, the results in this example should be considered as a simple proof-of-principle demonstration.

Fig. 4 shows several chosen projections cut from different parts of the overall MLA image plane 16 which was captured by the camera. As shown in this figure, the relative positions of the two letters change as a function of the location of the projection on the entire MLA image plane 16. This is the effect that leads to the 3-D properties of the hologram obtained at the end of the process. After capturing the MLA image plane 16 by the CCD camera 20, the processing stage was started by cutting each of the projections from the MLA image plane 16 and centering the projections on a chosen reference point. The cutting process was performed semi-automatically by detecting the first and the last elemental images in each row of the MLA image plane 16. Then, the distance between these two extreme elemental images was divided by the number of microlenses utilized in each row of the MLA 14 and the elemental images were cut from the MLA image plane 16 accordingly. Afterward, digital correlation with a known pattern taken from any of the elemental images was employed in order to fix a common reference point for all the elemental images. It is envisaged by the inventors that completely automatic cutting and centering methods may be possible.

In the experiment, the common reference point was chosen to be the center of the letter 'I'. The meaning of this process was setting the origin of the 3-D scene on the plane of the letter 'I'. Each of the projections was normalized (divided by its maximal value), multiplied, according to Eqs.

(1) and (2), by a linear phase function dependent on the position of this projection in the entire set of projections and then summed up into a single complex value in the Fourier hologram *H*. The magnitude and the phase of the Fourier hologram obtained in the experiment are shown in Figs. 5A and 5B, respectively. In order to digitally reconstruct the 3-D scene recorded into this hologram, a 2-D inverse Fourier transform was first applied to the 2-D complex matrix representing the hologram.

Fig. 5C shows the results of this inverse Fourier transform according to the present invention. In the reconstruction plane obtained by this operation, the letter 'I' is in focus, whereas the letter 'H' is out of focus. Then, a Fresnel propagation was applied to this reconstruction plane by convolving it with a quadratic phase [6]. The purpose of this propagation was to reveal other planes along the optical axis of the 3-D scene reconstruction. Fig. 5D shows the reconstruction in the best focus plane of the letter 'H'. In this figure, the letter 'I' is out of focus. This validates the fact that volumetric information is indeed encoded inside the hologram synthesized by the method of the present invention.

Alternative digital processes

One disadvantage of MVP holograms is the complication of acquiring the large number of viewpoint projections of the 3-D scene needed for generating a high resolution hologram. Another difficulty is the numerical

complexity and the inaccuracy of the digital process carried out on the acquired projections.

The method of the present invention provides a solution to both of the disadvantages. According to the recording stage of the present invention as described hereinabove, the multiple images of the 3-D scene are acquired by the use of a microlens array which acquires the entire set of viewpoint projections in a single camera shot. Following this, the second (processing) stage of the invention is carried out to yield a 2-D Fourier hologram of the 3-D scene.

However, this processing stage, illustrated hereinabove, can be carried out in many ways. First, both 1-D and 2-D MVP holograms can be generated. In case of a 1-D MVP hologram, the projections are acquired along a single axis only, and a multiplication by a 1-D phase function is performed, where the inner product sum is the corresponding column in the hologram matrix. In case of a 2-D MVP hologram, the projections are acquired along a two axes (2-D grid), and a multiplication by a 2-D phase function is performed, where the inner product sum is the corresponding pixel in the hologram matrix.

Second, by choosing a different phase function, or point spread function (PSF), we can create correlation holograms. However, in contrast to prior

art correlation holograms [7,8], the hologram of the present invention is produced under incoherent white light illumination. It is possible to define new types of digital holograms with certain advantages over the known types of holograms. The inventors have recently proposed a new MVP hologram called a digital incoherent Fresnel hologram (DIMFH) [9,10]. The DIMFH is generated by processing the MVPs directly, rather than performing a Fresnel propagation on the reconstruction of a Fourier hologram as done in the past [4,11]. Therefore, redundant calculations and digital errors during the various transformations are avoided. Furthermore, this direct Fresnel holography method is not limited to small angles and hence the hologram reconstruction is more accurate.

It is also possible to define another type of correlation hologram called digital incoherent protected correlation hologram (DIPCH) [10]. The reconstructed 3-D scene obtained from the DIPCH has a significantly improved transverse resolution compared to the 3-D scene reconstructed from the DIMFH, especially for the far objects in the scene. In addition to this feature, which is important for a wide variety of applications, the 3-D information encoded into the DIPCH is scrambled with a random PSF and thus the hologram can be used for encrypting the recorded 3-D scene. The general theoretical framework presented in this invention can be used for defining other types of new digital holograms for obtaining other advantages over the known types of digital holograms.

As explained above, any type of incoherent correlation holograms can be generated from the acquired projections and for each of the hologram types, both 1-D and 2-D correlation holograms can be synthesized.

One dimensional Hologram

For the 1-D incoherent correlation hologram, $2K+1$ projections of the 3-D scene along the horizontal axis only are acquired. The projections are numbered by m, so that the middle projection is denoted by $m = 0$, the right projection by $m = K$ and the left projection by $m = -K$. According to the method of this embodiment of the present invention, each horizontal line of the m-th projection $P_m(x_p, y_p)$ is multiplied by the same 1-D PSF and the product is summed into the (m,n)-th pixel in a complex matrix as follows:

$$H_1(m,n) = \iint P_m(x_p, y_p) E_1(x_p, y_p - n\Delta p) dx_p dy_p, \tag{12}$$

where $E_1(x_p, y_p)$ represents the generating PSF of the 1-D hologram, x_p and y_p are the axes on the projection plane, n is the row number in the complex matrix H_1 and Δp is the pixel size of the digital camera. $E_1(x_p, y_p)$ is defined as follows:

$$E_1(x_p, y_p) = A_1(bx_p) \exp[ig_1(bx_p)] \delta(y_p), \tag{13}$$

where A_1 and g_1 are general functions dependent on x_p only and may be defined differently for every type of the incoherent correlation hologram as

shown below. b is an adjustable parameter (with units that preserve the arguments of A_1 and g_1 as unitless quantities), δ is Dirac delta function. Additionally, the function $A_1(bx_p)\exp[-ig_1(bx_p)]$ has the property that its Fourier transform is a pure phase function. As shown in the following, this condition is necessary to guarantee that the hologram generated from this PSF can be reconstructed properly. According to Eq. (12), each projection contributes a different column to the complex matrix $H_1(m,n)$, which, as confirmed herein below, represents the 1-D incoherent correlation hologram of the 3-D scene.

To obtain the reconstructed plane, $s_1(m,n;z_r)$, located at an axial distance z_r from the 1-D correlation hologram, the hologram can be digitally convolved with a reconstructing PSF as follows:

$$s_1(m,n;z_r) = \left| H_1(m,n) * R_1(m;z_r) \right|, \tag{14}$$

where * denotes a 1-D convolution and $R_1(m;z_r)$ is the reconstructing PSF of the 1-D hologram defined as follows:

$$R_1(m;z_r) = A_1\left(\frac{m\Delta p}{z_r}\right)\exp\left[-ig_1\left(\frac{m\Delta p}{z_r}\right)\right]. \tag{15}$$

A_1 and g_1 are the same functions used for generating the PSF of the 1-D hologram [Eq. (13)].

Two Dimensional Hologram

The 2-D incoherent correlation hologram is synthesized from $(2K+1)$ horizontal by $(2K+1)$ vertical projections of the 3-D scene. The projections are numbered by m and n, so that the middle projection is denoted by $(m,n) = (0,0)$, the upper right projection by $(m,n) = (K,K)$ and the lower left projection by $(m,n) = (-K, -K)$. The (m,n)-th projection $P_{m,n}(x_p, y_p)$ is multiplied by a 2-D PSF and the product is summed to the (m,n)-th pixel in a complex matrix as follows:

$$H_2(m,n) = \iint P_{m,n}(x_p, y_p) E_2(x_p, y_p) dx_p dy_p, \tag{16}$$

where $E_2(x_p, y_p)$ represents the generating PSF of the 2-D hologram defined as follows:

$$E_2(x_p, y_p) = A_2(bx_p, by_p) \exp[ig_2(bx_p, by_p)], \tag{17}$$

A_2 and g_2 are general functions depending on (x_p, y_p) and may be defined differently for every type of incoherent correlation hologram as discussed below. Once more, the function $E_2(x_p, y_p)$ has the property that its Fourier transform is a pure phase function in order to enable a proper reconstruction as it is in the case of the 1-D hologram. The process manifested by Eq. (16) is repeated for all the projections, but in contrast to the 1-D case presented herein above, in the 2-D case, each projection contributes a single pixel to the hologram, rather than a column of pixels. In the end of this digital process, the obtained 2-D complex matrix

$H_2(m,n)$ represents the 2-D incoherent correlation hologram of the 3-D scene.

The reconstructed plane $s_2(m,n;z_r)$, located a distance z_r from the 2-D incoherent correlation hologram, is obtained by digitally convolving the hologram with a reconstructing PSF as follows:

$$s_2(m,n;z_r) = \left| H_2(m,n) * R_2(m,n;z_r) \right|, \tag{18}$$

where this time * denotes a 2-D convolution and $R_2(m,n;z_r)$ is the reconstructing PSF of the 2-D hologram, defined as follows:

$$R_2(m,n;z_r) = A_2\left(\frac{m\Delta p}{z_r}, \frac{n\Delta p}{z_r}\right)\exp\left[-ig_2\left(\frac{m\Delta p}{z_r}, \frac{n\Delta p}{z_r}\right)\right]. \tag{19}$$

A_2 and g_2 are the same functions used in the generating PSF of the 2-D hologram in Eq. (17).

Two examples of incoherent correlation holograms

This section presents two possible incoherent correlation holograms, the DIMFH [9,10] and the DIPCH [10], where each of which has certain advantages over the regular types of digital holograms. The only difference between the DIMFH and the DIPCH is the definition of the PSFs used in the generation and reconstruction of the hologram. More types of incoherent correlation holograms may be defined for gaining other advantages over the regular types of digital holograms, by using other PSFs.

Digital Incoherent Modified Fresnel Hologram (DIMFH)

The DIMFH is actually an incoherent Fresnel hologram generated directly by processing the MVPs of the 3-D scene. This direct method is faster and more accurate than the Fourier-based Fresnel holography methods [4,11], since redundant calculations and approximation errors are avoided. The generation and the reconstruction of the 1-D DIMFH is performed by Eqs. (12) and (14), respectively, where the generating PSF is a 1-D quadratic phase function given by:

$$E_1(x_p, y_p) = \exp\left(i2\pi b^2 x_p^{\,2}\right)\delta(y_p). \tag{20}$$

Similarly, the 2-D DIMFH processing is carried out by Eqs. (16) and (18), where the generating PSF is a 2-D quadratic phase function given by:

$$E_2(x_p, y_p) = \exp\left[i2\pi b^2 (x_p^{\,2} + y_p^{\,2})\right]. \tag{21}$$

Digital Incoherent Protected Correlation Hologram (DIPCH)

The DIPCH is a new type of incoherent correlation hologram which has two advantages over the Fresnel hologram in general and over the DIMFH in particular. First, since a constrained random PSF is used to generate the hologram, only an authorized user that knows this constrained random PSF can reconstruct the 3-D scene encoded into the hologram. Therefore, the DIPCH can be used as a method of encrypting the recorded 3-D scene. Second, the reconstruction obtained from the DIPCH has a significantly higher transverse resolution for far objects in the 3-D scene compared to the Fresnel hologram in general and to the DIMFH in

particular. In fact, far objects recorded by the DIMFH are reconstructed with a reduced transverse resolution because of two reasons: (a) Due to the parallax effect, far objects 'moves' slower throughout the projections, and therefore they sample a magnified version of the generating PSF. This magnified version has narrower bandwidth and therefore the reconstruction transverse resolution of far objects decreases in comparison to the closest object. (b) The quadratic phase used in the DIMFH has lower frequencies as one approaches its origin. Since far objects are correlated with the central part of the quadratic phase function along a range that becomes shorter as much as the object is more far away, the bandwidth of the DIMFH of far objects becomes even narrower beyond the bandwidth reduction mentioned in (a). In contrast to the DIMFH, the spatial frequencies of the DIPCH are distributed uniformly all over its area. Therefore, the DIPCH suffers from resolution reduction of far objects only due the reason (a). Hence, the images of far objects reconstructed from the DIPCH, besides of being protected by the constrained random PSF, also have higher transverse resolution.

The 1-D DIPCH process is still defined by Eqs. (12) and (14). However, this time, the generating PSF is a random function which fulfills the constraint that its Fourier transform is a pure phase function. In order to find this PSF, the projection is used onto the constraint sets (POCS)

algorithm [12,13]. The POCS algorithm used for finding this PSF is illustrated in Fig. 6. The POCS is an iterative algorithm which bounces from the PSF domain to its spatial spectrum domain and backward, using Fourier transform and its inverse transform. In each domain, the function is projected onto the constraint set. The two constraints of the POCS express the two properties required for the PSF of the DIPCH. First, the Fourier transform of the PSF should be a phase-only function. This requirement enables to reconstruct the DIPCH. Therefore, the constraint of the POCS in the spectral domain is the set of all phase-only functions and each transfer function is projected onto this constraint by setting its magnitude distribution to the constant 1. The other property of the PSF is that it should be space limited into a relatively narrow region close to but outside of the origin. This condition reduces the reconstruction noise from the out-of-focus objects because the overlap during the correlation between the resampled space-limited reconstructing PSF and the hologram at out-of-focus regions is lower than the case of using a wide-spread PSF. Of course, this noise is lower by as much as the existence region of the PSF is narrower. However narrowing the existence region makes it difficult for the POCS algorithm to converge to a PSF that satisfies both constraints with an acceptable error. In any event, the constraint set in the PSF domain is all of the complex functions that identically equal zero in any pixel outside the predefined narrow existence region. The projection onto the constraint set in the PSF domain is performed by multiplying the

PSFs by a function that is equal to 1 inside the narrow existence region of the PSF and 0 elsewhere. In the case of the 1-D DIPCH, the constrained PSF looks like a narrow strip of columns, whereas in the case of the 2-D DIPCH this PSF looks like a narrow ring. In the end of the process, the POCS algorithm yields the suitable constrained random PSF that can be used in the hologram generation process. Figs 7A and 7B show the resulting PSFs that can be used for generating the 1-D and the 2-D DIPCHs, respectively.

Next is shown that the resolution for far objects in the case of DIMFH is worse than in the case of DIPCH. For a single object point, the resulting hologram in the case of DIMFH is exactly the PSF given by Eq. (20) or (21). These expressions are actually equal to the transfer function of a lens, for which the resolution properties are well known. For a single point located a distance $z_{s,\min}$ from the imaging system, the width of the recorded hologram is $2K\alpha f/z_{s,\min}$, and the smallest resolved detail, as mentioned herein above, is $\alpha f/(Mz_{s,\min})$. Now, for a point located a distance z_s from the imaging system, the width of the recorded hologram is $2K\alpha f/z_s$. Since, as explained above, the DIMFH of an object point located in a distance z_s from the imaging system, is equivalent to a lens, the hologram resolving power is linear dependent on its width. Therefore, the resolved detail of an object at some distance z_s is the smallest ever resolved detail $\alpha f/(Mz_{s,\min})$ multiplied by the ratio between the maximum hologram width, $2K\alpha f/z_{s,\min}$,

and the actual hologram width, $2K\alpha f/z_s$. Hence the resolved detail of an object at some distance z_s is $\alpha f z_s/(Mz^2_{s,\min})$. The recalled size of the resolved object's detail in the case of DIPCH is $\alpha f/(Mz_{s,\min})$. Therefore, the ratio between the resolving power of the DIPCH and the DIMFH is $(z_s/z_{s,\min})$. Again, this means that as much as the object is far from $z_{s,min}$, the resolution power of the DIPCH over the DIMFH is better.

While this invention has been described in terms of specific examples, many modifications and variations are possible. It is therefore understood that within the scope of the appended claims, the invention may be realized otherwise than as specifically described.

REFERENCES

1. B. W. Schilling, T. -C. Poon, G. Indebetouw, B. Storrie, K. Shinoda, Y. Suzuki, and M. H. Wu, "Three-dimensional holographic fluorescence microscopy," Opt. Lett. **22**, 1506 (1997).

2. J. Rosen and G. Brooker, "Digital spatially incoherent Fresnel holography," Opt. Lett. (to be published).

3. D. Abookasis and J. Rosen, "Computer-generated holograms of three-dimensional objects synthesized from their multiple angular viewpoints," J. Opt. Soc. Am. A **20**, 1537 (2003).

4. Y. Sando, M. Itoh, and T. Yatagai, "Holographic three-dimensional display synthesized from three-dimensional Fourier spectra of real existing objects," Opt. Lett. 28, 2518 (2003).

5. T. Mishina, M. Okui, and F. Okano, "Calculation of holograms from elemental images captured by integral photography," Appl. Opt. **45**, 4026 (2006).

6. J. Goodman, *Introduction to Fourier Optics*, 2nd ed. (McGraw-Hill, New York, 1996), Chap. 5.

7. B. Javidi and A. Sergent, "Fully phase encoded key and biometrics for security verification," Opt. Eng. **36**, 935-942 (1997).

8. D. Abookasis and J. Rosen, "Digital correlation holograms implemented on a joint transform correlator," *Opt. Commun.* **225**, 31-37 (2003).

9. N. T. Shaked and J. Rosen, "Modified Fresnel computer generated hologram directly recorded by multiple viewpoint projections," Accepted for Publication to *Applied Optics - Special Issue on Digital Holography*. To be published.

10. N. T. Shaked and J. Rosen, "Multiple viewpoint projection holograms synthesized by spatially-incoherent correlation with a general function," Submitted.

11. D. Abookasis and J. Rosen, "Three types of computer-generated hologram synthesized from multiple angular viewpoints of a three-dimensional scene," *Appl. Opt.* **45,** 6533-6538 (2006).

12. J. R. Fienup, "Phase-retrieval algorithm: a comparison," *Appl. Opt.* **21,** 2758-2769 (1982).

13. H. Stark, *Image Recovery: Theory and Application*, Academic Press, Orlando (1987), pp. 29-78 and pp. 277-320.

CLAIMS

1. Method of obtaining a digital hologram of a three-dimensional (3-D) scene comprising the steps of:
    a. illuminating said scene with incoherent white-light;
    b. recording multiple projections of said 3-D scene; and
    c. computer processing of said projections by the performance of a predetermined sequence of mathematical operations;

characterized in that a microlens array (MLA) is used to create said multiple projections in an image plane which is projected onto the imaging sensor of a camera, thereby allowing the obtaining of all of said multiple projections in a single camera shot.

2. A method according to claim 1, wherein said predetermined sequence of mathematical operations comprise the steps of:
    a. cutting the single shot image received from said camera into a set of projections of said 3-D scene;
    b. centering said projections on the same reference point;
    c. multiplying said centered projections by linear phase functions; and
    d. summing each of said multiplied results into a single complex value yielding a complex matrix which represents a digital hologram.

3. A method according to claim 1, wherein said predetermined sequence of mathematical operations comprising the digital incoherent modified Fresnel hologram (DIMFH) method.

4. A method according to claim 1, wherein said predetermined sequence of mathematical operations comprising the digital incoherent protected correlation hologram (DIPCH) method.

5. System for obtaining a digital hologram of a three-dimensional (3-D) scene comprising:

   a. a source of incoherent white-light;
   b. a collimating lens;
   c. a microlens array (MLA);
   d. a focusing lens;
   e. a camera; and
   f. a computer

characterized in that:

   a. said MLA creates multiple images of said scene in the image plane of said MLA;
   b. said image plane is projected by said focusing lens onto the imaging sensor of said camera, thereby allowing the obtaining of all of said multiple projections of said scene in a single camera shot, which is transferred to said computer,

wherein predetermined sequence of mathematical operations is preformed on said projections to obtain said digital hologram.

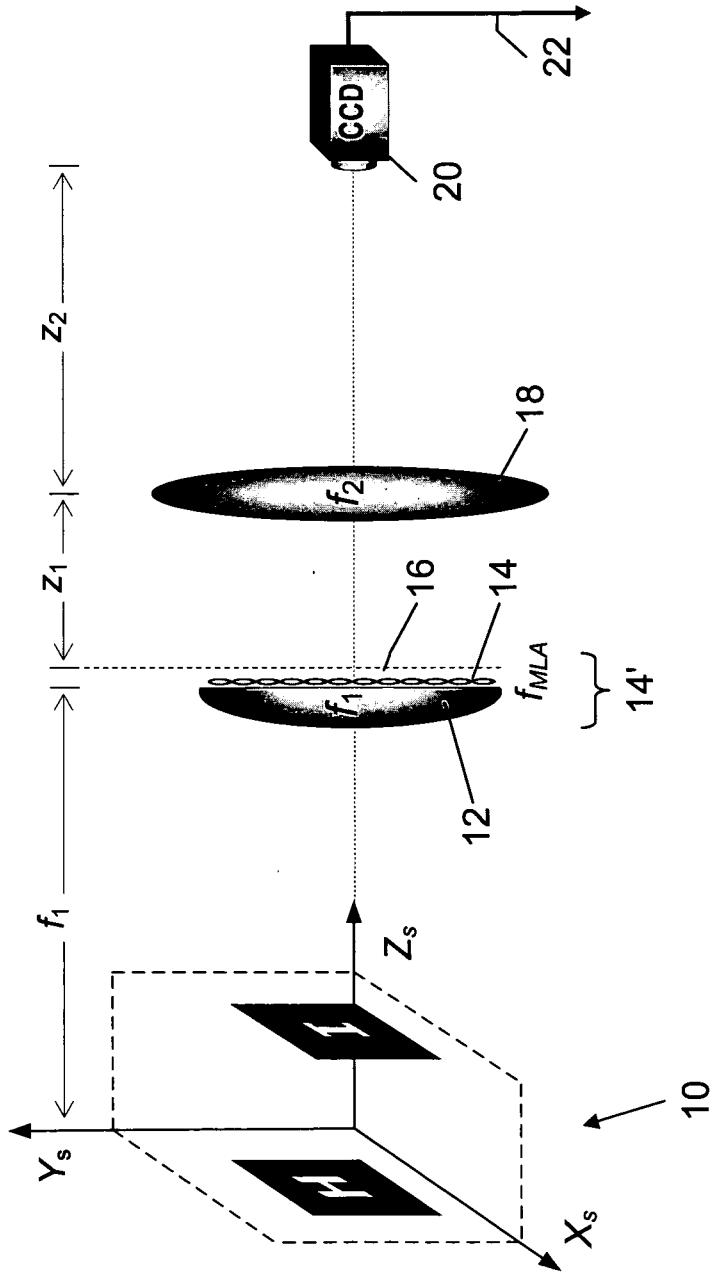

Fig. 1

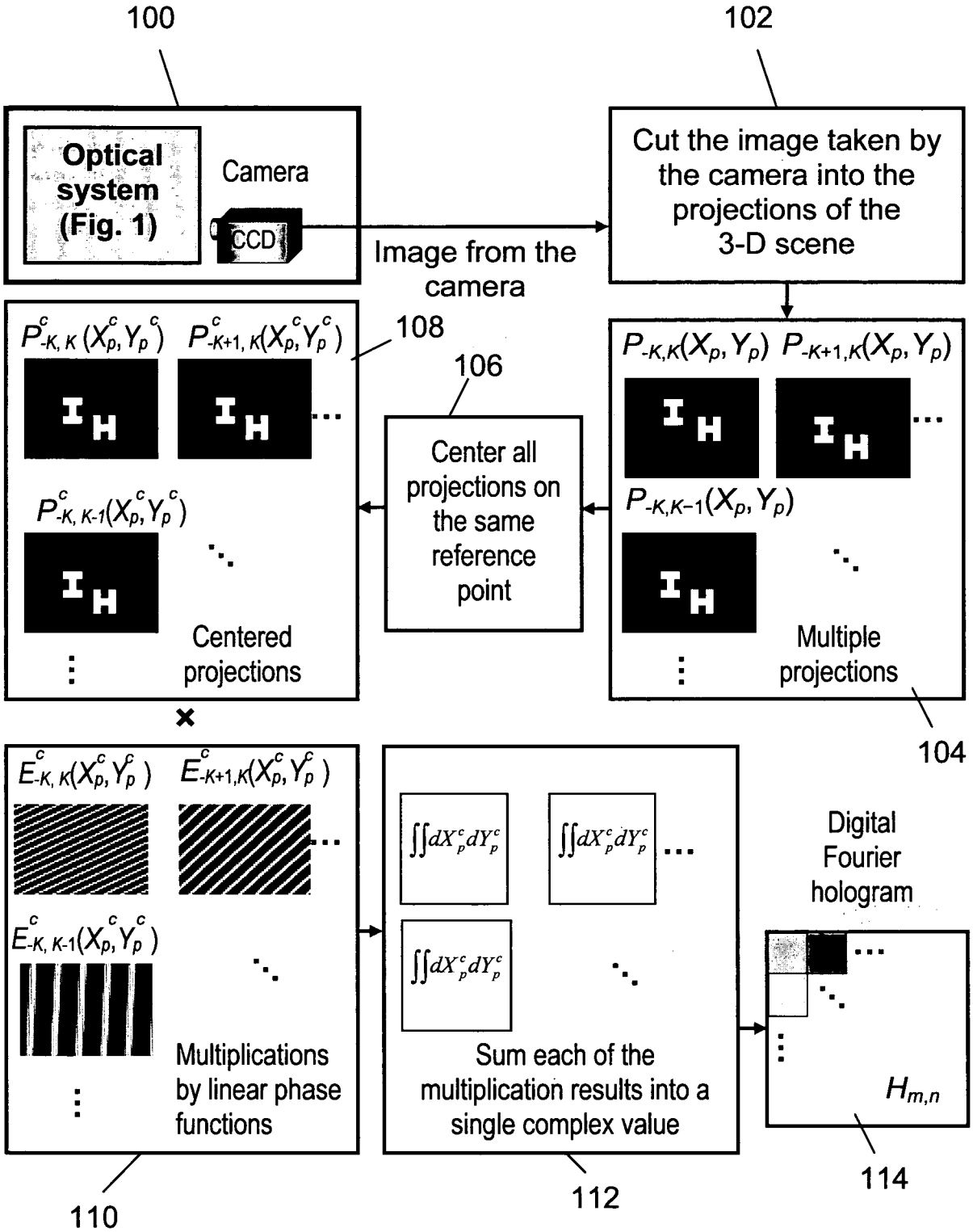
100
102
Optical system (Fig. 1)
Camera
CCD
Image from the camera
Cut the image taken by the camera into the projections of the 3-D scene
108
106
Center all projections on the same reference point
Centered projections
Multiple projections
104
Multiplications by linear phase functions
110
Sum each of the multiplication results into a single complex value
112
Digital Fourier hologram
$H_{m,n}$
114

Fig. 2

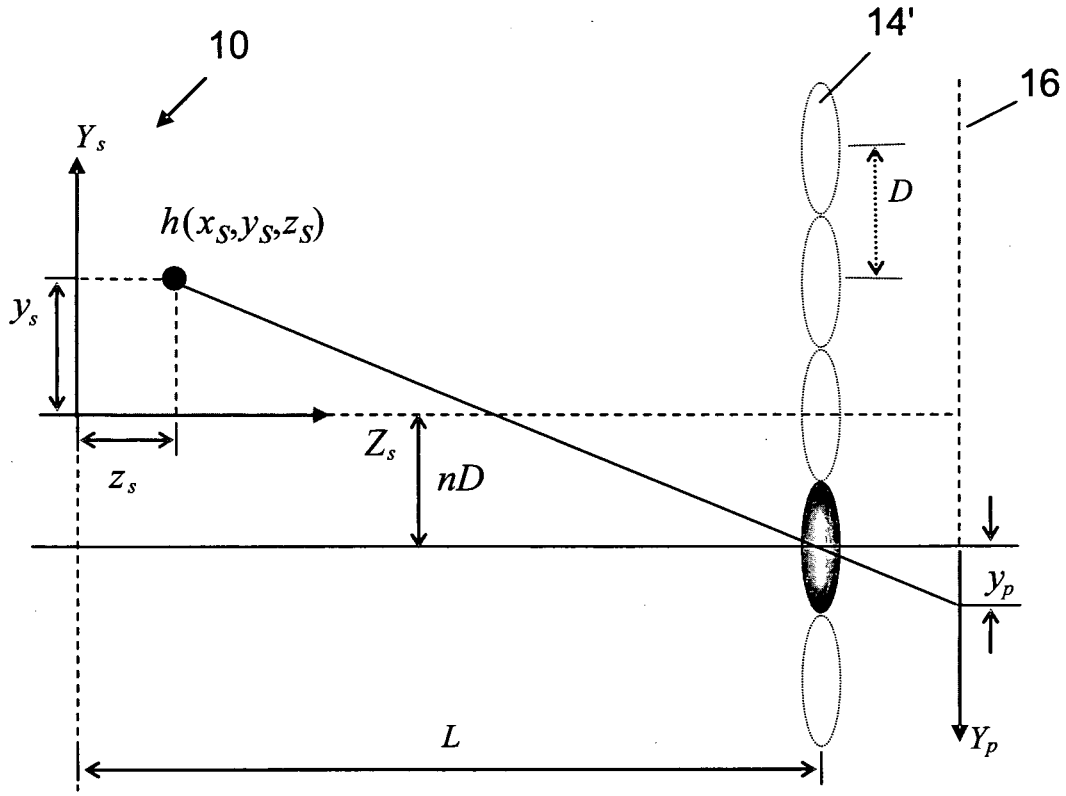

Fig. 3

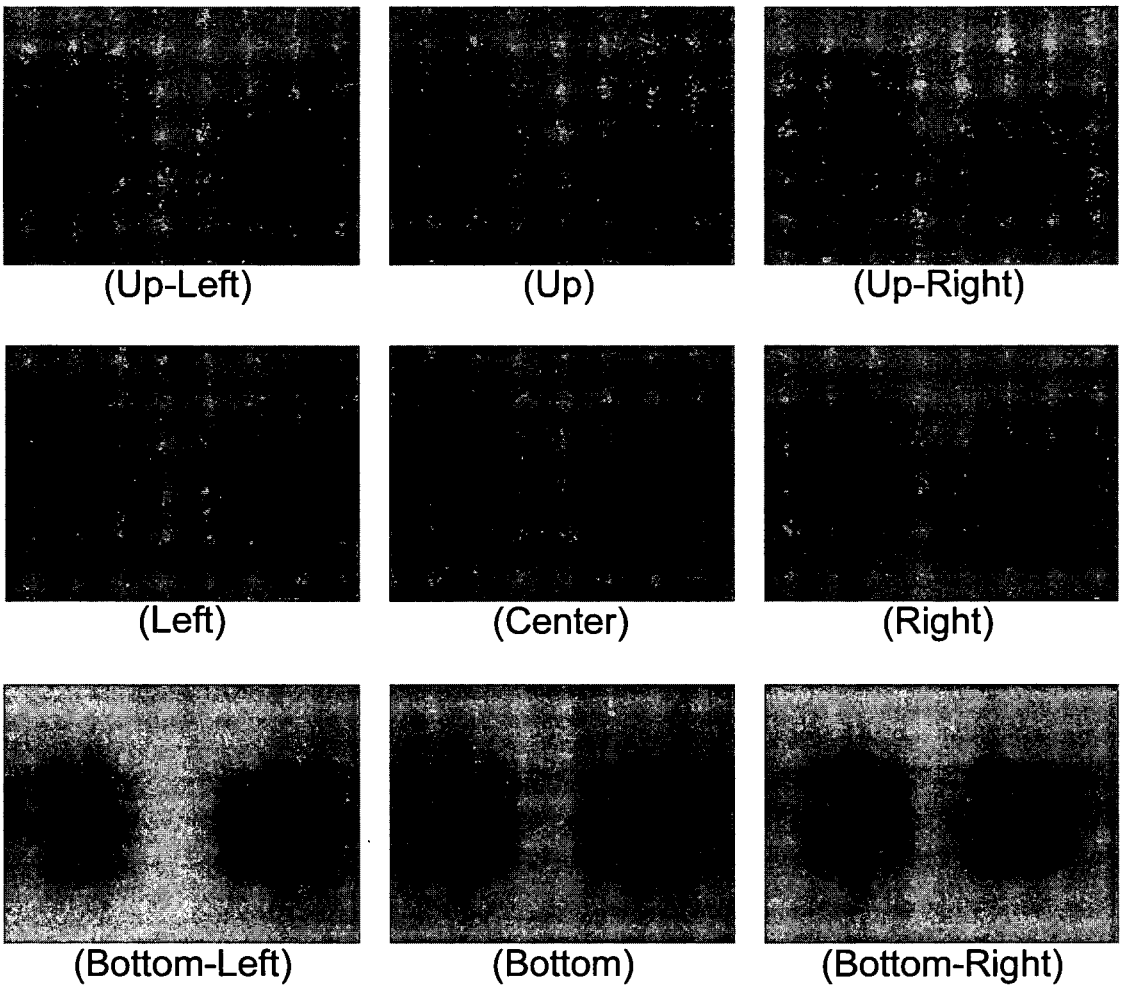

Fig. 4

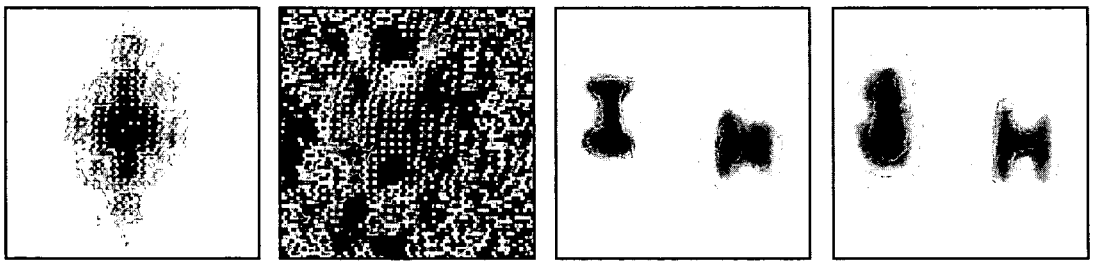

Fig. 5A Fig. 5B Fig. 5C Fig. 5D

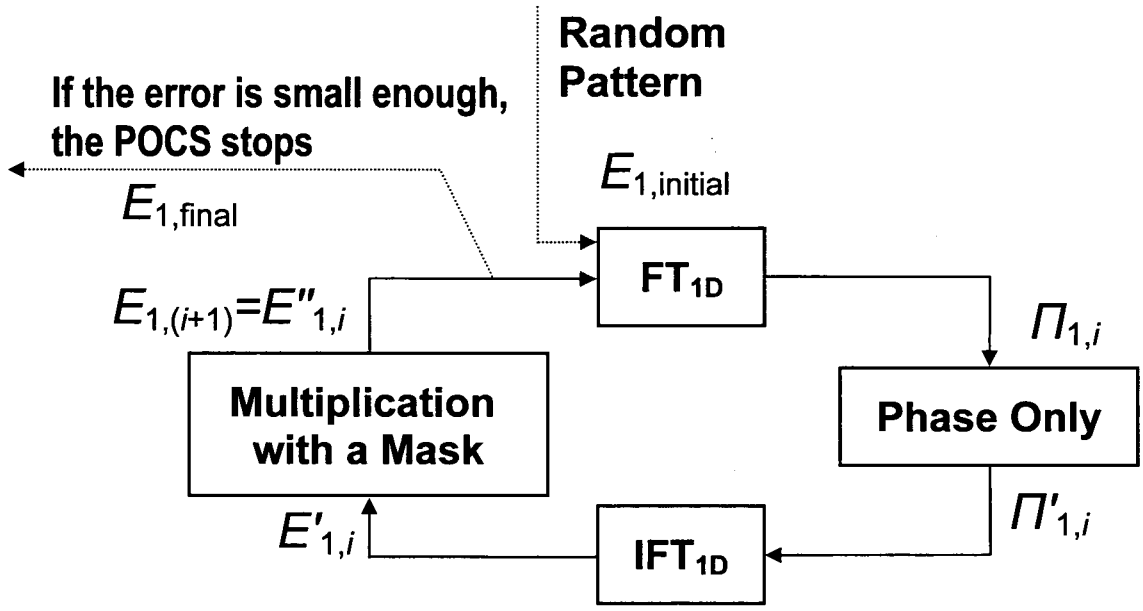
Random Pattern
If the error is small enough, the POCS stops
$E_{1,initial}$
$E_{1,final}$
$E_{1,(i+1)}=E''_{1,i}$
FT1D
$\Pi_{1,i}$
Multiplication with a Mask
Phase Only
$E'_{1,i}$
IFT1D
$\Pi'_{1,i}$

Fig. 6

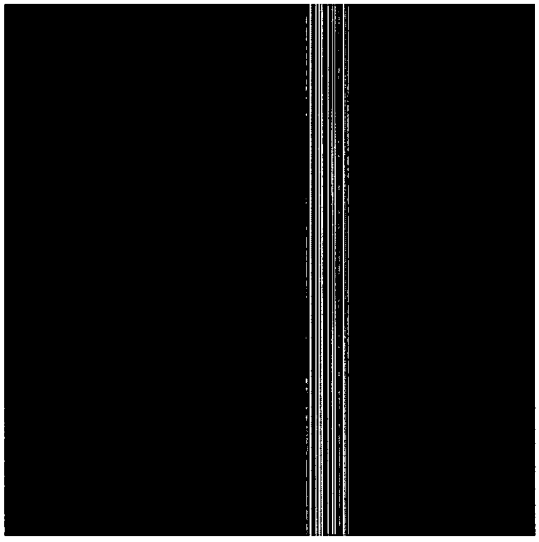

Fig. 7A

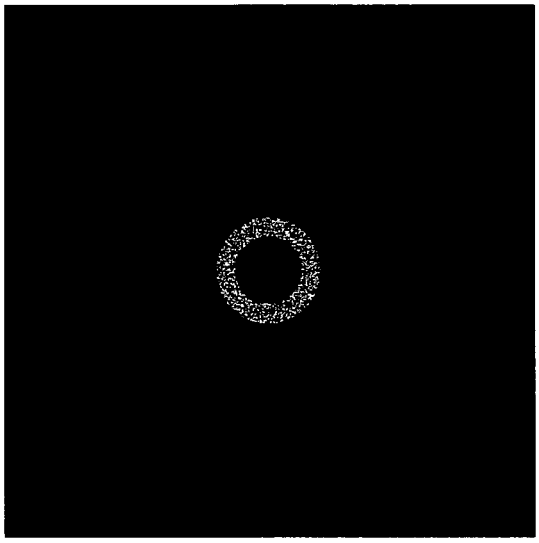

Fig. 7B